Acupuncture and Herbal Medicine

Integrated analysis of metabolomic and gut microbiota reveals idiosyncratic drug-induced liver injury resulting from the combined administration of bavachin and icariside II

Bo Cao[1], Yingying Li[1], Mengmeng Lin[1], Jing Xu[1], Taifeng Li[1], Xiaofei Fei[1], Xiaohe Xiao[2,*], Guohui Li[1,*], Chunyu Li[1,*]

[1]National Cancer Center/National Clinical Research Center for Cancer/Cancer Hospital, Chinese Academy of Medical Sciences and Peking Union Medical College, Beijing, China; [2]China Military Institute of Chinese Medicine, Fifth Medical Center of Chinese PLA General Hospital, Beijing, China

Abstract

Objective: Xianling gubao (XLGB), a widely used Chinese patent medicine for osteoporosis, has garnered significant attention due to its potential to cause liver injury. The constituents Psoraleae Fructus (PF, the dried ripe seeds of *Psoralea corylifolia L.*) and Epimedii Folium (EF, the dried leaves of various *Epimedium* species) present in XLGB have been implicated in causing idiosyncratic drug-induced liver injury (IDILI). However, the specific components and mechanisms underlying liver injury related to these tonics remain elusive. This study aims to establish that the combination of bavachin (the primary active compound in PF, and icariside II, the main active compound in EF) induces IDILI in a tumor necrosis factor-α (TNF-α)-mediated mouse model.

Methods: To assess the impact of bavachin and icariside II on the liver in the presence of TNF-α immune stress, an animal model was developed. Liquid chromatography-tandem mass spectrometry (LC-MS/MS) metabolomics technology was employed to identify biomarkers associated with TNF-α-induced IDILI and the combination of bavachin and icariside II. Additionally, 16S rRNA high-throughput sequencing technology was utilized to explore changes in the species composition and relative abundance of gut microbiota. Spearman correlation analysis was conducted to unveil the relationship between gut microbiota and *in vivo* metabolites.

Results: The study observed that the combined administration of bavachin and icariside II induced liver injury in the TNF-α mediated susceptibility mouse model of IDILI. Under TNF-α stimulation, there was an elevation in levels in mouse livers following bavachin and icariside II administration, while Gly-Tyr, Leu-Gly, and Trp-Ser levels decreased. These differentially expressed metabolites associated with liver injury were predominantly enriched in metabolic pathways such as sphingolipid metabolism, sphingolipid signaling pathway, and necroptosis. it is noteworthy that the gut of mice with liver injury induced by the bavachin and icariside II combination exhibited a significant increase in *Bacteroides* and *Desulfovibrionaceae* abundance. Correlation analysis revealed a positive association between *Bacteroidaceae* and *Desulfovibrionaceae* with methylcarbamoyl PAF and methyl Indole-3-acetate, while a negative correlation was observed with Gly-Tyr, Leu-Gly, and Trp-Ser.

Conclusions: These findings demonstrated that the combination of bavachin and icariside II increased the risk of IDILI *in vivo*, providing a promising scientific basis for understanding the component basis of IDILI resulting from the compatibility of EF and PF.

Keywords: Bavachin, Gut microbiota, Icariside II, IDILI, Metabolomics

Graphical abstract: http://links.lww.com/AHM/A97.

Introduction

Xianling gubao (XLGB), an oral preparation extensively used in China for bone diseases[1], has demonstrated efficacy[2,3] in clinical practice for over two decades. However, growing concerns about XLGB-induced liver injury have emerged, supported by an increasing number of reports[4]. In 2016, the China Food and Drug Administration (CFDA) emphasized the importance of monitoring and addressing adverse reactions related to XLGB-induced liver injury. A previous study revealed

Bo Cao and Yingying Li have contributed equally to this work.

**Corresponding author: Chunyu Li, E-mail: chunyu_li@126.com; Guohui Li, E-mail: lgh0603@cicams.ac.cn; Xiaohe Xiao, E-mail: pharmacy302xxh@126.com.*

Received 11 October 2023 / Accepted 31 January 2024

How to cite this article: *Cao B, Li YY, Lin MM, Xu J, Li TF, Fei XF, Xiao XH, Li GH, Li CY. Integrated analysis of metabolomic and gut microbiota reveals idiosyncratic drug-induced liver injury resulting from the combined administration of bavachin and icariside II. Acupunct Herb Med 2024;4(2):222–233. DOI: 10.1097/HM9.0000000000000099*

that while XLGB did not cause liver injury in normal rats, it induced noticeable damage in an immune stress model[5], highlighting its unique experimental properties. Despite this, the specific mechanisms linking inflammation-mediated immune stress to idiosyncratic liver injury caused by XLGB remain unknown and require further investigation.

Previous studies showed that tumor necrosis factor-α (TNF-α) is a critical factor, indicating that TNF-α-induced immune stress plays a pivotal role in XLGB-induced idiosyncratic drug-induced liver injury (IDILI)[5]. Investigations into the immunological mechanisms of IDILI show that TNF-α, combined with non-steroidal anti-inflammatory drugs like diclofenac sodium, activates the TNF-α-mediated mitogen-activated protein kinase/nuclear factor kappa-B (MAPK/NF-κB) signaling pathway, releasing numerous inflammatory cytokines[6]. Therefore, TNF-α-induced immune stress likely contributes significantly to the development of XLGB-induced IDILI.

Psoraleae Fructus (PF) consists of the dried ripe seeds of *Psoralea corylifolia L.*, while Epimedii Folium (EF) consists of the dried leaves of various *Epimedium* species[7,8]. These two herbal ingredients, commonly used tonics in traditional Chinese medicine (TCM), are often combined to treat osteoporosis and found in health food products[9,10]. This combination of psoralen and epimedium may activate the body's immune response, potentially contributing to XLGB-associated IDILI[11]. However, the specific components in PF leading to liver injury susceptibility and the immune susceptibility components in EF remain unclear, necessitating further exploration to understand the mechanisms underlying aggravated liver injury resulting from the combination of these two components. The main active component of PF, bavachin, triggers liver injury by activating the NLRP3 inflammasome in a mouse model through lipopolysaccharide mediation, highlighting its potential role in liver injury[11]. Similarly, icariside II from EF can induce idiosyncratic liver injury by enhancing NLRP3 inflammasome activation, suggesting its potential as an immune-susceptible factor contributing to liver injury[12].

Metabolomics, an innovative omics technology, has been widely applied to studying metabolite changes in organisms under stress[13,14], providing valuable insights into *in vivo* drug mechanisms[15]. The gut microbiota plays a crucial role in liver disease development[16], with disruptions in intestinal flora and barrier function leading to immune escape, impacting the liver. Consequently, disturbances in intestinal homeostasis alter immune status, resulting in chronic infections, immune insufficiency, and sterile liver inflammation due to excessive immune responses[17].

This study established a TNF-α immune stress animal model to assess the impact of bavachin and icariside II on mouse liver. Employing liquid chromatography-tandem mass spectrometry (LC-MS/MS) metabolomics and multivariate statistical analysis, we identified biomarkers associated with TNF-α-induced IDILI and the combination of bavachin and icariside II. Furthermore, 16S rRNA high-throughput sequencing identified key gut microbiota associated with IDILI induced by the combination of these compounds. These findings provide insights into the material basis and mechanism of IDILI caused by TCM compounds containing PF and EF, laying a scientific foundation for their rational clinical use.

Materials and methods

Chemicals and reagents

The mouse recombinant TNF-α (315-01A) was acquired from Peprotech Inc. (Rocky Hill, NJ, USA). Bavachin (19879-32-4, 99.97%) and icariside II (113558-15-9, 98.47%) were obtained from Chengdu Pufei De Biotech Co., Ltd (Chengdu, China) [Supplementary Figure S1, http://links.lww.com/AHM/A98]. Assay kits for the detection of plasma alanine aminotransferase (ALT) and lactate dehydrogenase (LDH) were sourced from Shanghai Enzyme-linked Biotechnology Co., Ltd. (Shanghai, China). Acetonitrile, Methyl tert-Butyl Ether (MTBE), formic acid, methanol, ammonium formate, and isopropanol (High Performance Liquid Chromatography [HPLC] grade) were supplied by Thermo Fisher Scientific Inc. (Beijing, China). All other reagents and solvents used were of the highest commercially available grade.

Animal handling and experimental design

Male Balb/c mice, aged 6 to 8 weeks and weighing 18 to 20 g [SCXK (Beijing) 2019-0010], were sourced from SPF Biotechnology Co., Ltd. (Beijing, China). All mice were given *ad libitum* access to standard food and pure water, and they were kept under a 12 h light/12 h dark cycle at a temperature of (25 ± 2)°C with moderate humidity. Housing and handling of the animals adhered to approved protocols by the Animal Experimental Ethics Committee of the National Cancer Center (NCC2023A406). The mice were randomly divided into eight groups (n = 6 per group): (1) Control (C), (2) TNF-α (T), (3) Bavachin (B), (4) Icariside II (I), (5) Bavachin + icariside II (BI), (6) TNF-α + bavachin (TB), (7) TNF-α + icariside II (TI), and (8) TNF-α + bavachin + icariside II (TBI). The entire experimental process is depicted in Figure 1A. Before any experiment, the mice were allowed to acclimate to the environment for a minimum of 7 d and were subjected to a 24-hour fasting period (Figure 1A). A single dose of TNF-α (10 μg/kg body weight, dissolved in saline water, i.v.) or vehicle (saline water) was administered. Two hours post-administration, bavachin (50 mg/kg, dissolved in 0.5% CMC-Na, p.o.) and/or icariside II (25 mg/kg, dissolved in 0.5% CMC-Na, p.o.) or their respective vehicle (0.5% CMC-Na, p.o.) were administered. After 16 h of TNF-α administration, the mice were sacrificed, and plasma samples and liver tissues were collected for further analysis.

Biochemical and histological examination

After centrifuging at 3,000 rpm for 20 min, ALT and LDH activities were measured using the provided directions for the assay kits. Liver tissues were fixed

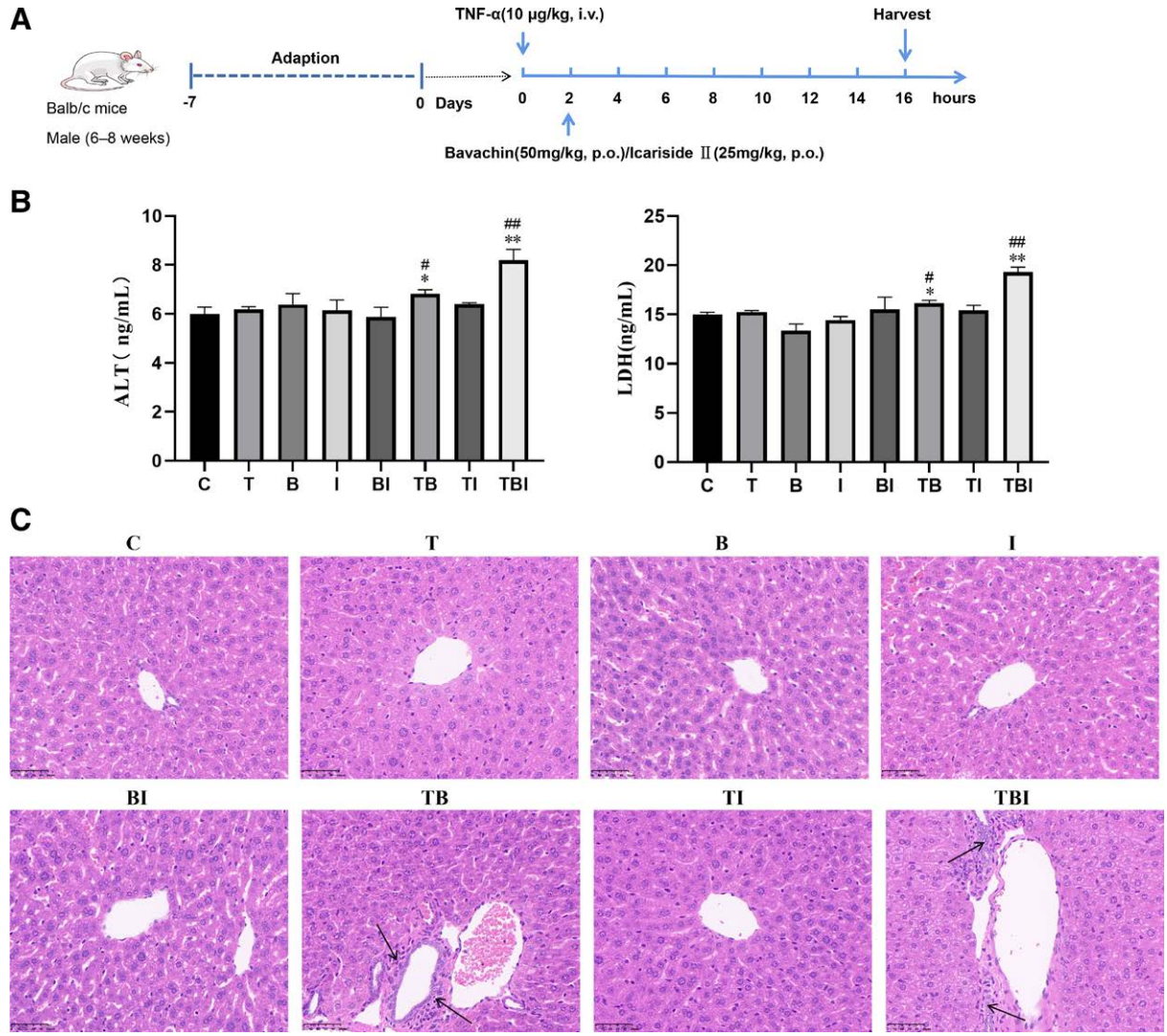

Figure 1. Effects of bavachin and/or icariside II administration on hepatic injury parameters with or without TNF-α prestimulation. (A) Schematic presentation of the experimental procedure to assess hepatotoxicity induced by bavachin + icariside II + TNF-α. (B) Levels of plasma ALT and LDH in mice treated with bavachin and/or icariside II with or without TNF-α pretreatment ($n = 6$), *$P < 0.05$ versus N, **$P < 0.01$ versus N, #$P < 0.05$ versus T, ##$P < 0.01$ versus T. (C) Representative pictures of liver tissue sections stained with H&E, analyzed by IHC (200×). ALT: alanine aminotransferase; B: Bavachin; BI: Bavachin + icariside II; C: Control; H&E: Hematoxylin and eosin; I: Icariside II; IHC: Immunohistochemistry; LDH: Lactate dehydrogenase; T: TNF-α; TB: TNF-α + bavachin; TBI: TNF-α + bavachin + icariside II; TI: TNF-α + icariside II; TNF-α: Tumor necrosis factor-α.

with 4% paraformaldehyde and embedded in paraffin. Subsequently, 4 μm slices were sectioned from paraffin tissue blocks, and liver injury extent was assessed using hematoxylin and eosin (H&E) staining.

Liver metabolomics analysis

Liver tissues, weighing approximately 20 mg, were homogenized with a steel ball for 20 seconds, followed by centrifugation at 3,000 rpm for 30 seconds at 4°C. The resulting mixture was combined with a 1 mL solution containing MTBE:methanol (3:1, v/v) and an internal standard mixture, whirling for 15 min. Next, 200 μL of water was added, and the mixture was whirled for 1 min before being centrifuged at 12,000 rpm for 10 min at 4°C. A 200 μL supernatant was extracted, concentrated until dry, and then dissolved in a 200 μL mixture of acetonitrile and isopropanol (1:1, v/v), whirling for 3 min and centrifuging (12,000 rpm, 3 min, and 4°C). The sample extracts were analyzed using an LC-ESI-MS/MS system (UPLC [SCIEX ExionLC AD, USA], and MS [SCIEX QTRAP 6500+, USA]) with the following conditions: UPLC column - Waters ACQUITY UPLC HSS T3 C_{18} (1.8 μm, 2.1 mm × 100 mm); column temperature, 40°C; flow rate, 0.4 mL/min; injection volume, 2 μL; solvent system, water (0.1% formic acid): acetonitrile (0.1% formic acid); gradient program, 95:5 V/V at 0 min, 10:90 V/V at 11.0 min, 10:90 V/V at 12.0 min, 95:5 V/V at 12.1 min, 95:5 V/V at 14.0 min. Linear ion trap (LIT) and triple quadrupole (QQQ) scans were acquired using a triple quadrupole-LIT mass spectrometer (QTRAP), QTRAP® LC-MS/MS System, equipped with an ESI Turbo Ion-Spray interface, operating in positive and negative ion mode and controlled by Analyst 1.6.3 software (Sciex). The ESI source operation parameters were as follows: source temperature 500°C; ion spray voltage (IS) 5,500 V (positive), −4,500 V (negative); ion source gas I (GSI), gas II (GSII), curtain gas (CUR) set at 55, 60, and 25.0 psi, respectively; collision gas (CAD) set to high. Instrument tuning and mass calibration were performed using 10 and 100 μmol/L polypropylene glycol solutions in QQQ and LIT modes, respectively. A specific

set of multiple reaction monitoring (MRM) transitions were monitored for each period based on the eluted metabolites. Different groups were compared using OrthogonalPartialLeast Squares-DiscriminantAnalysis (OPLS-DA), permutation test, and S-plot analysis conducted with SIMCA Software. Differential metabolites were screened based on variable importance in projection (VIP) scores >1 and P value < 0.05 (Student t test). Other relative metabolism analysis was conducted and analyzed at Wuhan Metware Biotechnology Co., Ltd (Wuhan, China).

16S rRNA sequencing

An average of six fecal samples were collected from each group, and total microbial DNA was extracted using the E.Z.N.A.® soil DNA kit according to the provided instructions. DNA quality and concentration were assessed through 1.0% agarose gel electrophoresis and a NanoDrop® ND-2000 spectrophotometer (Thermo Scientific, USA). Polymerase chain reaction (PCR) amplification of the V3 to V4 variable region of bacterial 16S rRNA was carried out with 338F and 806R primers. The resulting amplification products were purified, pooled, and paired for sequencing on the Illumina MiSeq PE300 platform, following standard operating procedures. DADA2 denoised sequences, referred to as amplicon sequence variants (ASVs), were obtained. Taxonomic assignment of ASVs utilized the Naive Bayes consensus taxonomy classifier in Qiime2 and the SILVA 16S rRNA database (v138). Data analysis and processing were conducted using the Majorbio Cloud Platform (http://www.majorbio.com).

Statistical analysis

The data were analyzed using GraphPad Prism 9.0 software and are presented as mean ± standard deviation (SD). The one-way analysis of variance (ANOVA) was used to evaluate the significance among the three groups. The t test was utilized for comparisons between two groups. Statistical significance was set at $P < 0.05$, signifying a significant difference, and $P < 0.01$, indicating a highly significant difference.

Results

The co-administration of bavachin and icariside II exacerbates hepatotoxicity under TNF-α-mediated immunological stress conditions

The hepatotoxicity of bavachin and/or icariside II *in vivo* was demonstrated through the administration of recombinant TNF-α. In Figure 1B, mice in the T group exhibited unchanged plasma ALT and LDH activities compared with the control group, indicating no hepatic injury from this TNF-α dose alone ($P > 0.05$). Treatment with isolated bavachin or icariside II alone or in combination did not significantly elevate plasma ALT and LDH activities compared with the C or T groups ($P > 0.05$). Moreover, TNF-α-exposed mice treated with icariside II alone did not show a significant difference in plasma ALT and LDH activities compared with both the C and T groups ($P > 0.05$). However, TNF-α-exposed mice treated with bavachin alone exhibited a significant difference compared with both the C and T groups ($P < 0.05$). Co-administration of bavachin and icariside II under TNF-α prestimulation led to a substantial increase in ALT and LDH activities compared with all other treatment groups in mice ($P < 0.01$). Additionally, co-exposure to TNF-α, bavachin, and icariside II resulted in pathological changes, including inflammatory cell infiltration in portal areas, loss of central vein intima, and hepatocyte focal necrosis (Figure 1C). Inflammatory cell infiltration in portal areas was also observed in the BI group. These changes were either not observed or only minimally present in the C, T, B, I, BI, or TI group. In summary, the combination of bavachin and icariside II induces hepatic injury in the TNF-α-mediated susceptibility mouse model.

Effects of bavachin combined with icariside II on liver metabolome under TNF-α-mediated immunological stress conditions

To explore variations in metabolites across the C, T, TB, TI, and TBI groups, we utilized OPLS-DA for comprehensive classification and discriminant analysis. The OPLS-DA scores clearly demonstrated the distinction between the C and T groups in both positive ion mode (Figure 2A) and negative ion mode [Supplementary Figure S2A, http://links.lww.com/AHM/A98]. Model parameters derived in positive ion mode (C *vs.* T group: R2X = 0.563, R2Y = 0.9999, and Q2 = 0.783) underscored the model's high interpretability and predictive capability. A random permutation test ($n = 200$) substantiated the model's effectiveness, with the left side of the positive ion R2 and Q2 values for the C and T groups consistently lower, affirming non-overfitting and robust predictive ability (Figure 2B). Identification of differential metabolites relied on a VIP value of ≥1.0 and a significant P value ($P < 0.05$) from a Student t test (Figure 2C). To gain deeper insights into the relevant metabolic pathways in the TNF-α-mediated susceptibility mouse model of IDILI, we integrated identified differential metabolites into the Kyoto Encyclopedia of Genes and Genomes (KEGG) database for pathway analysis. The results unveiled the involvement of these metabolites in glycerophospholipid (GP) metabolism, choline metabolism in cancer, and glycine, serine, and threonine metabolism (Figure 2D), signifying dysregulation in multiple pathways associated with the TNF-α-mediated susceptibility mouse model's progression. Similar distinct patterns emerged in the TB and TBI groups, as well as the TI and TBI groups, with evident separation in both positive ion mode (Figure 3A and D) and negative ion mode [Supplementary Figure S2B and C, http://links.lww.com/AHM/A98]. Model parameters in positive ion mode (TB *vs.* TBI group: R2X = 0.44, R2Y = 0.982, and Q2 = 0.296; TI *vs.* TBI group: R2X = 0.542, R2Y = 0.98, and Q2 = 0.632) underscored the OPLS-DA model's high interpretability and predictive capability. The random permutation test ($n = 200$) further validated the model's effectiveness, with consistent lower left-side positive ion R2 and Q2 values for the TB and TBI groups, as well as

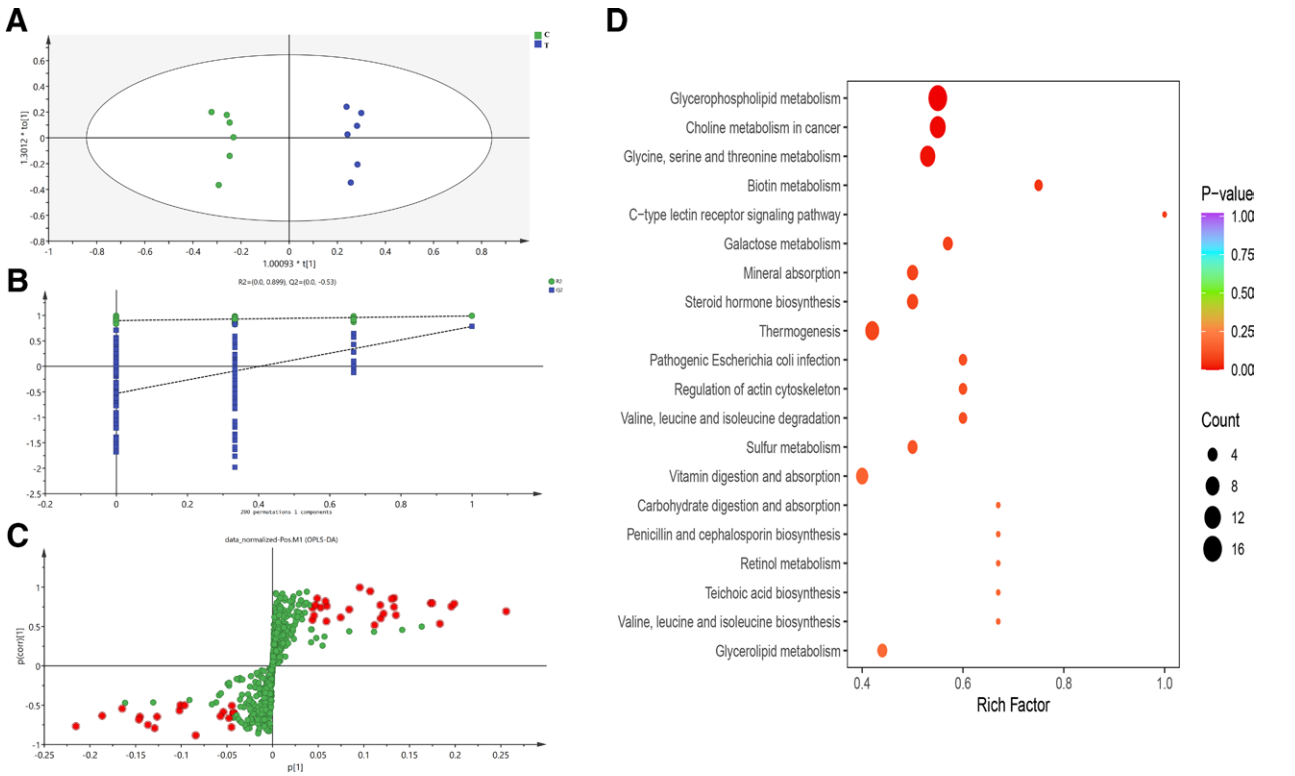

Figure 2. Changes in metabolic levels of control and TNF-α exposure in mouse liver. (A) OPLS-DA score plots of the C and T groups in mouse liver in ESI + mode. (B) Evaluation of the OPLS-DA models through response permutation tests in ESI + mode (n = 200). (C) S-score plots constructed from supervised OPLS analysis of liver in ESI + mode. (D) KEGG enrichment analysis of differentially expressed metabolites between the C and T groups, showing the top 20 pathways with lipid pathway enrichment. C: Control; ESI: Electrosprayionization; KEGG: Kyoto Encyclopedia of Genes and Genomes; OPLS-DA: OrthogonalPartialLeast Squares-DiscriminantAnalysis; T: TNF-α; TNF-α: Tumor necrosis factor-α.

the TI and TBI groups (Figure 3B and E). Metabolites with VIP ≥ 1.0 and P value <0.05 were considered differential metabolites (Figure 3C and F). To identify variables associated with liver injury influenced by the synergistic effect of susceptibility factors and drugs, we conducted a Venn diagram analysis on the differential metabolites in the N, T, TB, TI, and TBI groups. By comparing differential variables between the TB and TBI groups with those between the TI and TBI groups and combining them with the differential variables between the C and T groups, we identified 32 exclusive differential variables between the TB, TI, and TBI groups [Figure 3G and H, Supplementary Table S1, http://links.lww.com/AHM/A98]. This exclusivity suggests that these variables are uniquely influenced by the synergistic effect of TNF-α and drugs, making them potential variables associated with liver injury. To further unveil the relevant metabolic pathways in drug-induced liver injury, we incorporated the 32 differential metabolites into the KEGG database and conducted pathway analysis. The results pointed to the involvement of these metabolites in sphingolipid metabolism, sphingolipid signaling pathway, necroptosis, and apoptosis, indicating the dysregulation of multiple pathways in the progression of liver injury (Figure 3I).

Moreover, we analyzed the trend of relative content changes in differential metabolites associated with liver injury. We identified metabolites with a significant upward or downward trend in the TBI group compared with the other four groups (C, T, TB, and TI groups). The results, presented in Figure 4, demonstrated that, in contrast to the other groups, 17 of the 32 differential metabolites exhibited significant increases or decreases in the TBI group (P < 0.5). The TBI group displayed significant upregulation of 12 differential metabolites, including methylcarbamyl PAF, Xanthine, (S)-Leucic acid, among others. Conversely, the TBI group exhibited significant downregulation of five differential metabolites, such as Pro-Gln, Leu-Gly, Gly-Tyr, among others.

Impact of the combination of bavachin and icariside II on gut microbiota diversity and composition under TNF-α-mediated immunological stress conditions

To further elucidate the mechanism of liver injury induced by the combination of bavachin and icariside II in the presence of TNF-α, we conducted 16S rRNA gene sequencing to investigate variations in the composition of gut microbiota among experimental mice. The dynamics of species abundance and community evenness were unveiled through rank-abundance curves, where the width symbolized species richness, and smoothness denoted evenness in the sample. Remarkably, our study illuminated distinct differences in rank-abundance curves among groups, particularly with the TBI group exhibiting the shortest width horizontally. This observation underscores the significant impact of administering bavachin and icariside II on the species richness of gut microbiota in mice (Figure 5A).

To further investigate the microbial landscape, we employed principal coordinate analysis (PCoA) and non-metric multidimensional scaling (NMDS). These analyses brought forth significant differences in the

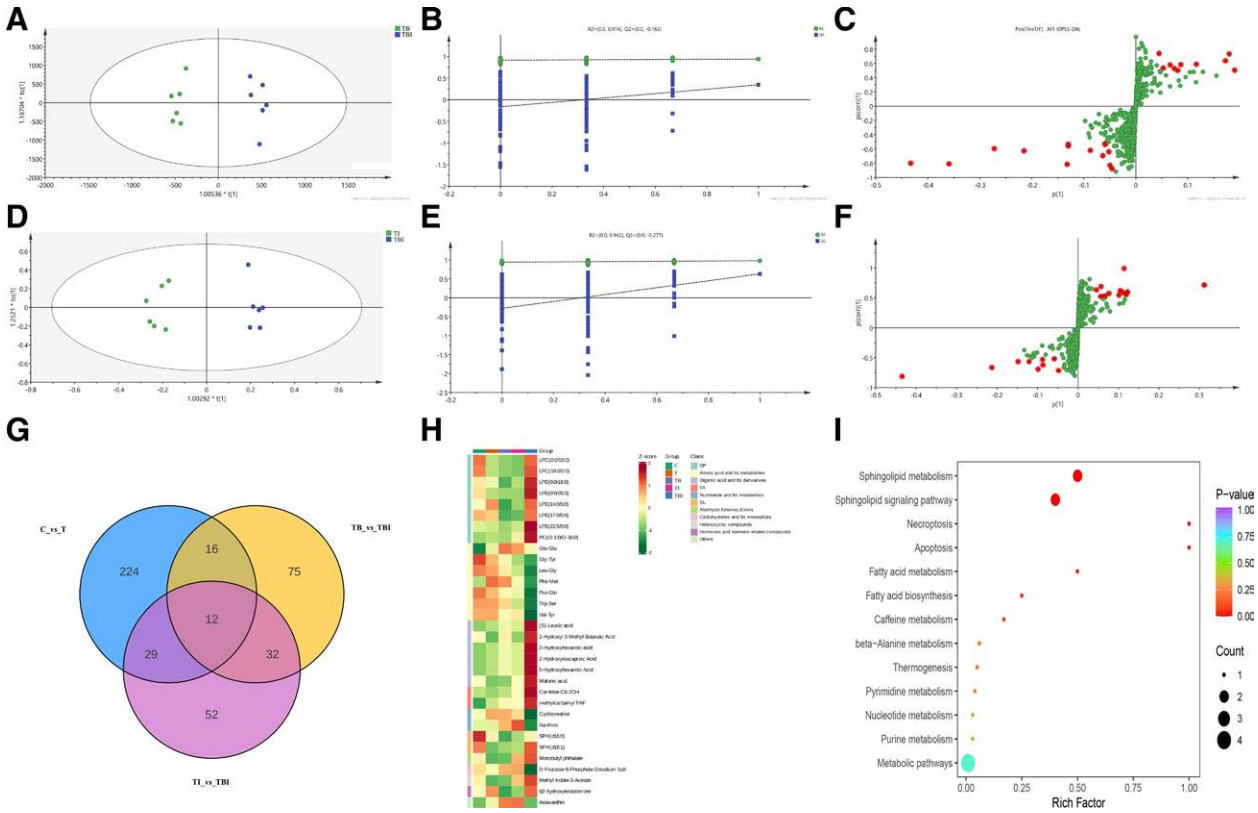

Figure 3. Metabolic changes in liver injury caused by the synergistic effect of TNF-α and bavachin + icariside II in mouse liver. (A), (D) OPLS-DA score plots of the TB and TBI groups, the TI and TBI groups in mouse liver in ESI + mode. (B), (E) Evaluation of the OPLS-DA models through response permutation tests in ESI + mode (n = 200). (C), (F) S-score plots constructed from supervised OPLS analysis of liver in ESI + mode. (G) Venn diagram of differentially expressed metabolites identified between the C versus T groups, the TB versus TBI groups, and the TI versus TBI groups. (H) Cluster heat map of differential metabolites. The horizontal axis represents the sample name, the vertical axis represents the differential metabolite information, the Group indicates the grouping, and the different colors represent different values obtained after standardization of relative contents (red represents high content, green represents low content). (I) KEGG enrichment analysis of differentially expressed metabolites between the C versus T groups, the TB versus TBI groups, and the TI versus TBI groups, showing the top 20 pathways with lipid pathway enrichment. C: Control; ESI: Electrosprayionization; KEGG: Kyoto Encyclopedia of Genes and Genomes; OPLS-DA: OrthogonalPartialLeast Squares-DiscriminantAnalysis; T: TNF-α; TB: TNF-α + bavachin; TBI: TNF-α + bavachin + icariside II; TI: TNF-α + icariside II; TNF-α: Tumor necrosis factor-α.

composition of intestinal microbial communities between the normal group and each intervention group (P = 0.001). Notably, the TBI group exhibited a greater dissimilarity from the normal group compared with the T, TB, or TI groups (Figure 5B and C). In summary, the administration of bavachin and icariside II resulted in a significant alteration in the composition of the intestinal microflora in mice.

For a deeper exploration of species composition at the phylum and genus levels, we conducted statistical analyses on the proportions of sequences at these levels relative to the total number of sequences in each sample, based on absolute abundance and annotation information. The gut microbiota composition at the phylum level revealed a distinct classification trend across the five groups, with notable differences in *Firmicutes* and *Bacteroidota* among the N, T, TB, TI, and TBI groups (Figure 5D and E). Dominant species at the genus level, such as *norank_f_Muribaculaceae*, *g_Lachnospiraceae_NK4A136_group*, and *unclassified_f_Lachnospiraceae*, were elucidated in the five mouse groups (Figure 5F and G). The Kruskal-Wallis H test was used to evaluate the significance of species abundance differences, with *Bacteroides* exhibiting higher abundance in the TBI group ($P < 0.05$). Moreover, the abundance of *norank_f_Desulfovibrionaceae* significantly increased following the administration of bavachin and icariside II in combination with TNF-α ($P < 0.01$). Furthermore, the abundance of *Candidatus_Saccharimonas* was significantly lower in the combination treatment group compared with the other four groups ($P < 0.05$) (Figure 6A).

Linear discriminant analysis (LDA) effect size (LEfSe) is a valuable tool in identifying specific species characteristics that delineate differences among multiple sample groups. We employed LEfSe with an LDA threshold of 4 to determine the key bacterial genera influencing liver injury in mice treated with the combination of bavachin and icariside II with TNF-α. The analysis unveiled five genera exhibiting significant differences: *g_Bacteroides*, *g_norank_f_Desulfovibrionaceae*, *g_Parabacteroides*, *g_Bilophila*, and *g_unclassified_f_Rikenellaceae* (Figure 6B).

Correlations between differential metabolites and differential gut microbiota in mice with liver injury

To investigate the potential relationship between liver injury-induced metabolic changes and gut microbiota, we conducted a Spearman correlation analysis between 17 differential metabolites identified in liver metabolomics and 5 differential bacteria identified

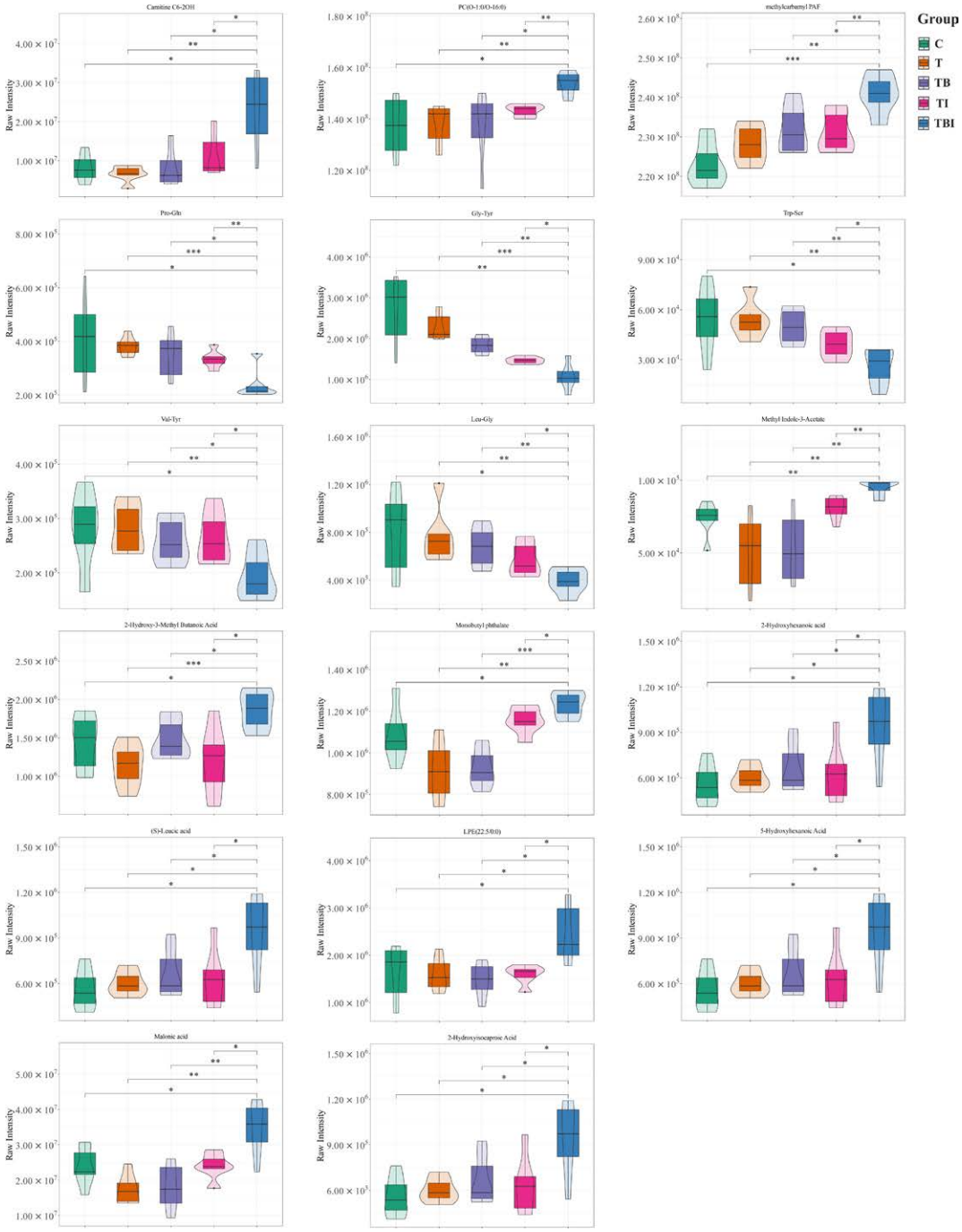

Figure 4. Violin plot showing the significant difference in metabolites. The x-axis represents the grouping, and the y-axis represents the relative content of differential metabolites (original peak area). *P < 0.05 versus TBI, **P < 0.01 versus TBI. TBI: TNF-α + bavachin + icariside II.

through LDA analysis, Figure 7 presents noteworthy associations. Methylcarbamyl PAF positively correlated with *Bacteroides*, *norank_f_Desulfovibrionaceae*, *Parabacteroides*, and *g_unclassified_f_Rikenellaceae*. Trp-Ser exhibited a negative correlation with *Bacteroides* and *Parabacteroides*. Phosphatidylcholine (PC) (O-1:0/O-16:0) demonstrated a positive correlation with *unclassified_f_Rikenellaceae*. Methyl indole-3-acetate showed a positive correlation with *Bacteroides*, *Parabacteroides*, and *Bilophila*. *Leu-Gly* revealed a negative correlation with *Bacteroides* and *Parabacteroides*. Finally, Gly-Tyr exhibited a negative correlation with *Bacteroides*, *norank_f_Desulfovibrionaceae*, *Parabacteroides*, and *g_unclassified_f_Rikenellaceae*.

Discussion

In recent years, growing apprehension has arisen over IDILI associated with TCM, particularly the use of traditional non-toxic Chinese medicine. Clinical prescriptions commonly incorporate both PF and EF, both classified as traditional tonic Chinese medicines. Concerns have been raised, supported by reports indicating that the combination of PF and EF may lead to IDILI[2,11]. Specifically, the

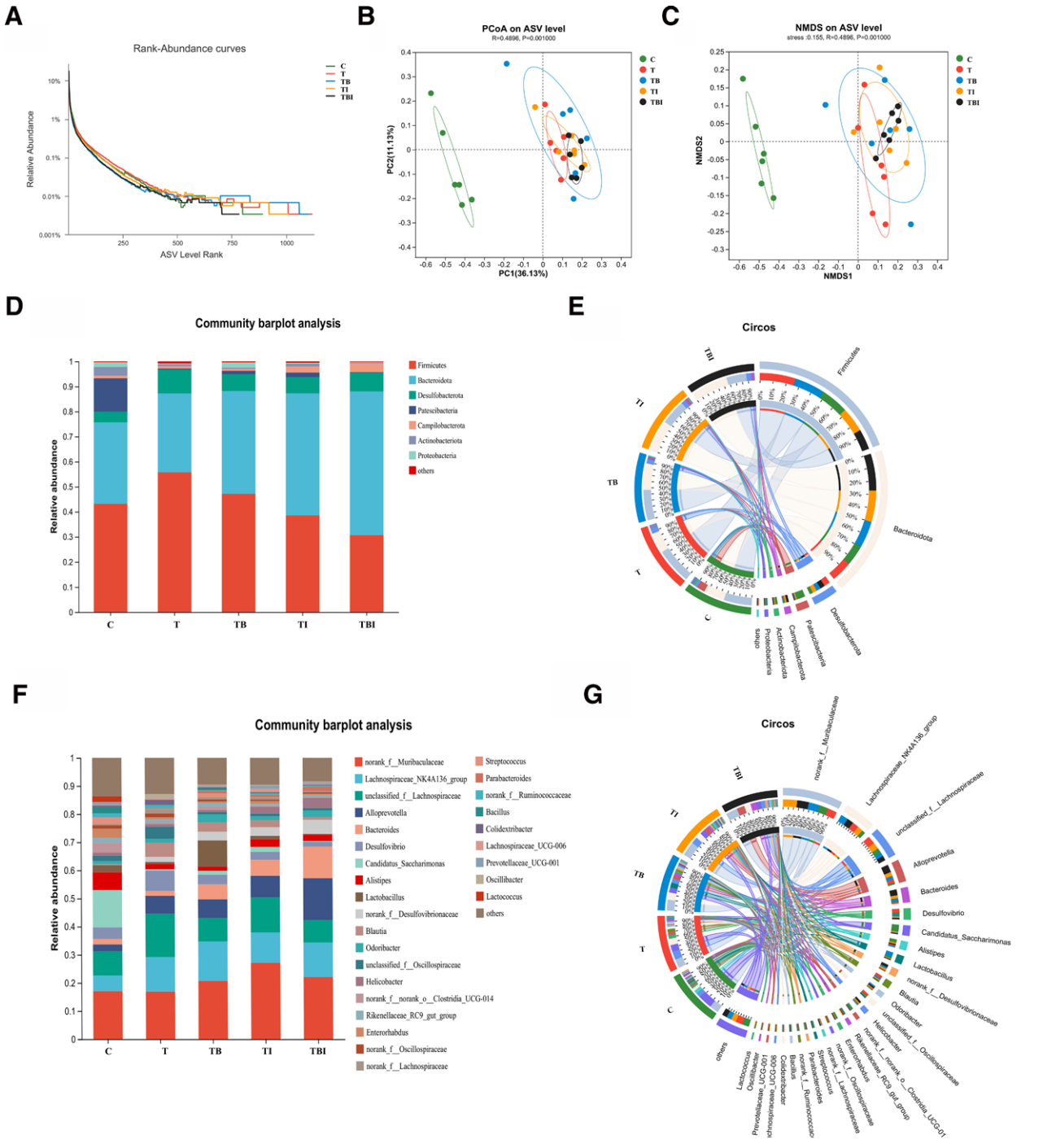

Figure 5. Changes in gut microbiota among the C, T, TB, TI, and TBI groups. (A) Rank-abundance curves. (B), (C) PCoA plots and NMDS of β-diversity at the ASV level. (D), (F) Relative abundance of bacterial communities at the phylum level and genus level. (E), (G) Community Circos diagram at the phylum level and genus level. ASV: Amplicon sequence variant; C: Control; NMDS: Non-metric multidimensional scaling; PCoA: Principal coordinate analysis; T: TNF-α; TB: TNF-α + bavachin; TBI: TNF-α + bavachin + icariside II; TI: TNF-α + icariside II.

primary active components of PF and EF, bavachin, and icariside II, respectively, have been implicated in IDILI. However, it remains unclear whether the concurrent use of bavachin and icariside II exacerbates hepatotoxicity and the underlying mechanism. Our study provides evidence that the combination of bavachin and icariside II indeed intensifies hepatotoxicity by influencing metabolites and gut microbiota[12,18]. Therefore, the combination of bavachin and icariside II emerges as a pivotal factor contributing to the aggravation of liver injury when PF and EF are employed together.

The intricate interconnection between metabolism and immunity is vital for the normal functioning of the body, with the metabolic state of immune cells playing a pivotal role in determining their functionality[19]. This study delves into the potential susceptibility mechanism of drug-induced liver injury from a metabolic perspective. Despite the absence of liver injury phenotypes induced by the immune stress susceptibility factor (TNF-α) in mice, our experimental results, obtained through metabolomics analysis, revealed significant alterations in 281 variables. Pathway enrichment analysis highlighted

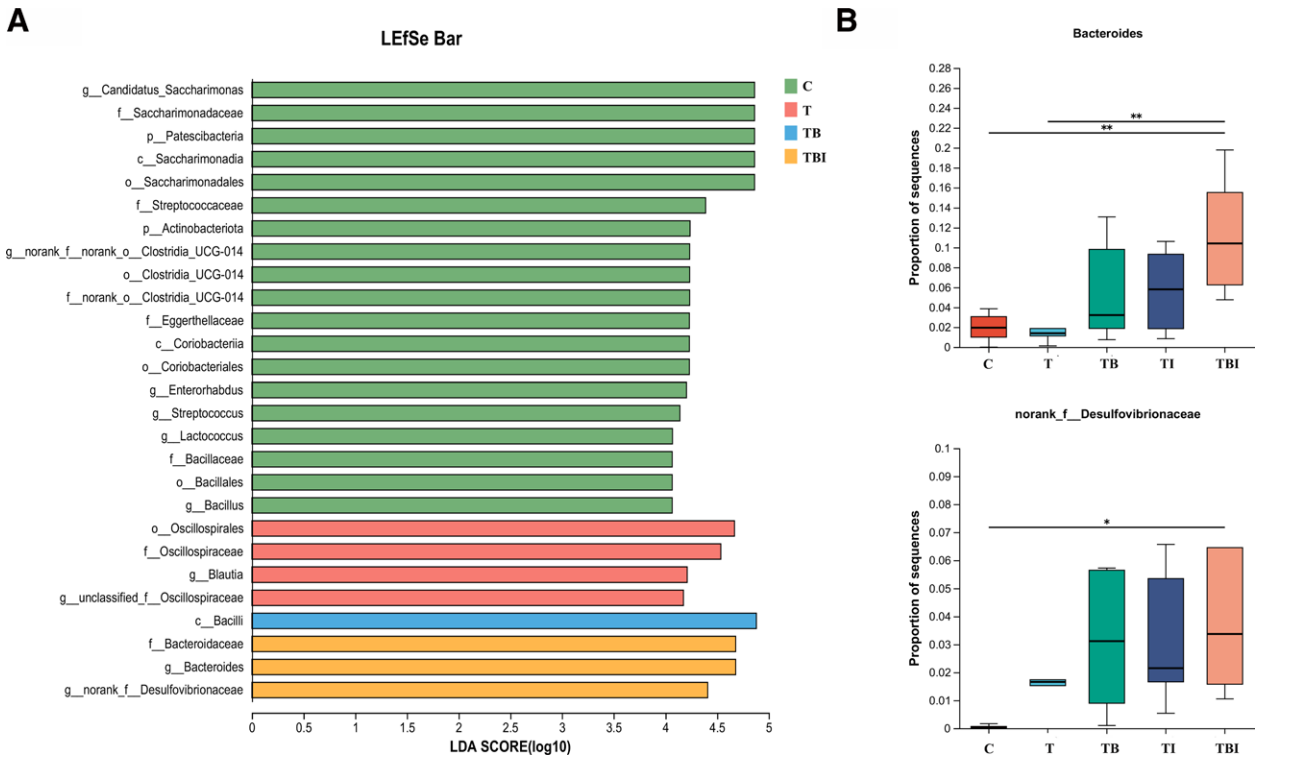

Figure 6. Analysis of species differences among the C, T, TB, TI, and TBI groups. (A) LDA discriminant histogram. LDA score threshold above 4. (B) Box plot of differential gut microbiota in the TBI group. C: Control; LDA: Linear discriminant analysis; LEfSe: Linear discriminant analysis effect size; T: TNF-α; TB: TNF-α + bavachin; TBI: TNF-α + bavachin + icariside II; TI: TNF-α + icariside II.

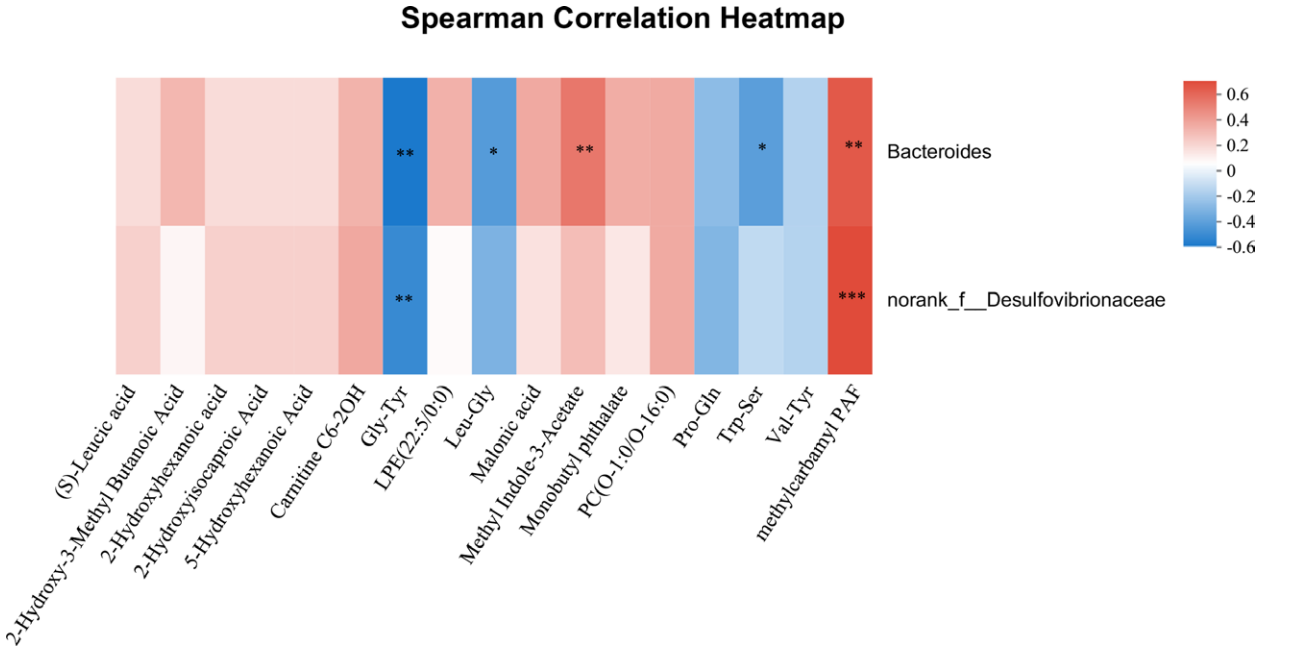

Figure 7. Correlation heatmap showing the relationship between 17 significant difference metabolites and 2 gut microbiota in the TBI group. TBI: TNF-α + bavachin + icariside II.

specific metabolic characteristics distinguishing the susceptible group (T group) from the control group (C group). Notably, glycophospholipid metabolism, choline metabolism in cancer, and glycine, serine, and threonine metabolism emerged as primary pathways. This unique state of metabolic reprogramming may serve as a crucial internal mechanism mediating the susceptibility factors of drug-induced liver injury. In particular, GP metabolism, recognized as characterizing the phenotype of drug-induced liver injury[20], showed a significant elevation in lysophosphatidylcholine (LPC) levels in the T group. LPC, a key pro-inflammatory lipid metabolite, plays a pivotal role in the inflammatory response[21]. The accumulation of LPC can lead to mitochondrial dysfunction and induce hepatocyte apoptosis[22,23]. Additionally, the increase in phosphocholine content in the T group,

associated with inflammatory stress, serves as an endogenous biomarker for cancer[24]. Despite the absence of apparent inflammatory reactions and liver injury phenotypes resulting from immune stress susceptibility factors, the altered metabolic state shifts the body's immune function towards a pro-inflammatory state, increasing susceptibility to drug-induced liver injury. This underscores the synergistic effect between susceptibility factors and drugs in causing liver injury. Expanding on immune stress susceptibility factors, the combination of bavachin and icariside II leads to significant increases in plasma levels of ALT and LDH, along with extensive infiltration of inflammatory immune cells and reactions in liver tissue. Further analysis of the metabolomic characteristics of the liver injury phenotype reveals significant changes in the metabolic profile of the TBI group compared with the TB and TI groups. Importantly, these changes differ from those caused by susceptibility factors alone. To eliminate the sole influence of TNF-α on the body, we subtracted the differing variables between the N and T groups from the common differing variables of the TB versus TBI and TI versus TBI groups. This approach allowed us to identify 32 variables associated with liver injury under the synergistic effect of susceptibility factors and drugs. The TBI group exhibited the highest content of GP compounds, including Lysophosphatidylethanolamine (LPE) (22:5/0:0) and PC(O-1:0/O-16:0), suggesting their role as the material basis for exacerbating liver injury under conditions of immune stress. Furthermore, metabolite identification and pathway enrichment analysis demonstrated that the metabolomic characteristics of liver injury induced by bavachin and icariside II primarily involve changes in metabolic pathways such as sphingolipid metabolism, sphingolipid signaling pathway, necroptosis, and apoptosis. Increasing evidence supports the notion that sphingolipid metabolism and the subsequent disruption of sphingolipid homeostasis play a key role in hepatocyte death and contribute to the onset and progression of various liver diseases, including viral hepatitis, ischemia-reperfusion injury, and steatohepatitis, among others[25–27].

The interplay among the liver, gastrointestinal tract, and intestinal microbial community is encapsulated in the gut-liver axis[28]. Recent studies link diseases like non-alcoholic fatty liver disease and alcoholic liver disease to changes in the gut microbiota's structure and function. Dysbiosis in the intestinal commensal community can trigger immune responses, including those affecting the host liver[29]. In this study, 16S rRNA gene sequencing was used to analyze microbial community abundance and intergroup differences, identifying five distinct bacteria at the genus level in the TBI group mice: *g_Bacteroides*, *g_norank_f_Desulfovibrionaceae*, *g_Parabacteroides*, *g__Bilophila*, and *g_unclassified_f_Rikenellaceae*. These findings suggest a crucial role of these bacteria in liver injury induced by the combination of bavachin and icariside II under immune stress. Notably, *g_Bacteroides* and *g_norank_f_Desulfovibrionaceae* were more abundant in the TBI group, with *g_Bacteroides*, generally considered beneficial, closely associated with liver disease development[30,31]. Studies indicate a significant increase in *g_Bacteroides* abundance in non-alcoholic steatohepatitis patients[32]. Conversely, *g_norank_f_Desulfovibrionaceae*, an opportunistic pathogen linked to inflammation, was highly abundant in conditions like non-alcoholic steatohepatitis, liver-associated liver cancer, and colitis[33–35]. Thus, the combination of bavachin and icariside II under immune stress conditions leads to liver injury by disrupting the intestinal flora balance, favoring harmful bacteria.

Microbial flora and metabolic correlation analysis unveiled the relationship between key intestinal flora and potential metabolites associated with liver injury at the genus level. Methylcarbamyl PAF and indole-3-acetate exhibited positive correlations with both *Bacteroides* and *Desulfovibrionaceae,* while Gly-Tyr, Leu-Gly, and Trp-Ser showed negative correlations with *Bacteroidaceae* and *Desulfovibrionaceae*. Platelet-activating factor (PAF), a lipid mediator, can induce platelet activation[36]. PAF binding to its receptor triggers cascade reactions, leading to oxidative stress, inflammatory response, and liver cell damage through multiple pathways[37,38]. Indole-3-acetate, closely associated with Bifidobacterium and Bacteroides[39], requires further investigation to understand its relationship with inflammation or liver injury. The liver's vital role in amino acid metabolism influences various diseases, including liver injury, cardiovascular disease, and diabetes[40–42]. Gly is an amino acid that benefits the liver by protecting liver cells and reducing damage[43–45]. Consistent with previous reports, the levels of Gly, Leu-Gly, and Trp-Ser decreased in the TBI group in this study.

Conclusion

Our study showed an elevated risk of IDILI *in vivo* with the combined use of bavachin and icariside II. Metabolomics and 16S rRNA sequencing analysis unveiled their impact on lipid, amino acid, and various metabolic pathways. These compounds also influenced the abundance of gut microbiota in *Bacteroidaceae* and *Desulfovibrionaceae*, culminating in liver injury. Therefore, our findings point to bavachin and icariside II as potential contributors to the aggravation of IDILI when combined with PF and EF, emerging as crucial factors in its development.

Conflict of interest statement

Xiaohe Xiao is an editorial board member of the journal. None of the other authors declare any conflicts of interest.

Funding

This work was supported by the National Natural Science Foundation of China (82174071).

Author contributions

Bo Cao and Yingying Li carried out the experiments, performed data analysis, and wrote the manuscript. Mengmeng Lin and Jing Xu analyzed the data. Taifeng Li and Xiaofei Fei performed parts of the experiments. Chunyu Li, Guohui Li, and Xiaohe Xiao designed the study and polished the manuscript.

Ethical approval of studies and informed consent

Animal procedures were performed in accordance with the National Institutes of Health guide for the care and use of laboratory animals, which was approved by the Scientific Investigation Board of the Cancer Hospital, Chinese Academy of Medicine Sciences, and related ethical regulations of Peking Union Medical College. And the Animal Experimental Ethics Committee of the National Cancer Center (NCC2023A406).

Acknowledgments

None.

Data availability

The original contributions presented in the study are included in the article/supplementary material; further inquiries can be directed to the corresponding authors.

References

[1] Cheng Y, Liu Y, Wang H, et al. A 26-week repeated dose toxicity study of Xian-ling-gu-bao in Sprague-Dawley rats. *J Ethnopharmacol* 2013;145:85–93.
[2] Wu H, Zhong Q, Wang J, et al. Beneficial effects and toxicity studies of Xian-ling-gu-bao on bone metabolism in ovariectomized rats. *Front Pharmacol* 2017;8:273.
[3] Li ZR, Cheng LM, Wang KZ, et al. Herbal Fufang Xian Ling Gu Bao prevents corticosteroid-induced osteonecrosis of the femoral head-a first multicentre, randomised, double-blind, placebo-controlled clinical trial. *J Orthop Translat* 2018;12:36–44.
[4] Wu W, Wang T, Sun B, et al. Xian-Ling-Gu-Bao induced inflammatory stress rat liver injury: inflammatory and oxidative stress playing important roles. *J Ethnopharmacol* 2019;239:111910.
[5] Li CY, Niu M, Liu YL, et al. Screening for susceptibility-related factors and biomarkers of Xianling Gubao capsule-induced liver injury. *Front Pharmacol* 2020;11:810.
[6] Giustarini G, Huppelschoten S, Barra M, et al. The hepatotoxic fluoroquinolone trovafloxacin disturbs TNF- and LPS-induced p65 nuclear translocation *in vivo* and *in vitro*. *Toxicol Appl Pharmacol* 2020;391:114915.
[7] Li YG, Hou J, Li SY, et al. Fructus Psoraleae contains natural compounds with potent inhibitory effects towards human carboxylesterase 2. *Fitoterapia* 2015;101:99–106.
[8] Ma H, He X, Yang Y, et al. The genus Epimedium: an ethnopharmacological and phytochemical review. *J Ethnopharmacol* 2011;134:519–541.
[9] Chopra B, Dhingra AK, Dhar KL. Psoralea corylifolia L. (Buguchi) - folklore to modern evidence: review. *Fitoterapia* 2013;90:44–56.
[10] Chen XJ, Tang ZH, Li XW, et al. Chemical constituents, quality control, and bioactivity of Epimedii Folium (Yinyanghuo). *Am J Chin Med* 2015;43:783–834.
[11] Gao Y, Wang Z, Tang J, et al. New incompatible pair of TCM: Epimedii Folium combined with Psoraleae Fructus induces idiosyncratic hepatotoxicity under immunological stress conditions. *Front Med* 2020;14:68–80.
[12] Wang Z, Xu G, Wang H, et al. Icariside II, a main compound in Epimedii Folium, induces idiosyncratic hepatotoxicity by enhancing NLRP3 inflammasome activation. *Acta Pharm Sin B* 2020;10:1619–1633.
[13] Johnson CH, Ivanisevic J, Siuzdak G. Metabolomics: beyond biomarkers and towards mechanisms. *Nat Rev Mol Cell Biol* 2016;17:451–459.
[14] Wang M, Chen L, Liu D, et al. Metabolomics highlights pharmacological bioactivity and biochemical mechanism of traditional Chinese medicine. *Chem Biol Interact* 2017;273:133–141.
[15] Liao Y, Wang C, Gao Z, et al. Anti-obesity mechanism of Ganpu tea revealed by microbiome, metabolome and transcriptome analyses. *Food Chem* 2023;412:135048.
[16] Albillos A, de Gottardi A, Rescigno M. The gut-liver axis in liver disease: pathophysiological basis for therapy. *J Hepatol* 2020;72:558–577.
[17] Wang R, Tang R, Li B, et al. Gut microbiome, liver immunology, and liver diseases. *Cell Mol Immunol* 2021;18:4–17.
[18] Qin N, Xu G, Wang Y, et al. Bavachin enhances NLRP3 inflammasome activation induced by ATP or nigericin and causes idiosyncratic hepatotoxicity. *Front Med* 2021;15:594–607.
[19] Próchnicki T, Latz E. Inflammasomes on the crossroads of innate immune recognition and metabolic control. *Cell Metab* 2017;26:71–93.
[20] Quintás G, Martínez-Sena T, Conde I, et al. Metabolomic analysis to discriminate drug-induced liver injury (DILI) phenotypes. *Arch Toxicol* 2021;95:3049–3062.
[21] Dennis EA, Norris PC. Eicosanoid storm in infection and inflammation. *Nat Rev Immunol* 2015;15:511–523.
[22] Hollie NI, Cash JG, Matlib MA, et al. Micromolar changes in lysophosphatidylcholine concentration cause minor effects on mitochondrial permeability but major alterations in function. *Biochim Biophys Acta* 2014;1841:888–895.
[23] Kakisaka K, Cazanave SC, Fingas CD, et al. Mechanisms of lysophosphatidylcholine-induced hepatocyte lipoapoptosis. *Am J Physiol Gastrointest Liver Physiol* 2012;302:G77–G84.
[24] Glunde K, Jacobs MA, Bhujwalla ZM. Choline metabolism in cancer: implications for diagnosis and therapy. *Expert Rev Mol Diagn* 2006;6:821–829.
[25] Li L, Wang H, Jones JW. Sphingolipid metabolism as a marker of hepatotoxicity in drug-induced liver injury. *Prostaglandins Other Lipid Mediat* 2020;151:106484.
[26] Nojima H, Freeman CM, Gulbins E, et al. Sphingolipids in liver injury, repair and regeneration. *Biol Chem* 2015;396:633–643.
[27] Kwong EK, Li X, Hylemon PB, et al. Sphingosine kinases/sphingosine 1-phosphate signaling in hepatic lipid metabolism. *Curr Pharmacol Rep* 2017;3:176–183.
[28] Bauer KC, Littlejohn PT, Ayala V, et al. Nonalcoholic fatty liver disease and the gut-liver axis: exploring an undernutrition perspective. *Gastroenterology* 2022;162:1858–1875.e2.
[29] Woodhouse CA, Patel VC, Singanayagam A, et al. Review article: the gut microbiome as a therapeutic target in the pathogenesis and treatment of chronic liver disease. *Aliment Pharmacol Ther* 2018;47:192–202.
[30] Zhu L, Baker SS, Gill C, et al. Characterization of gut microbiomes in nonalcoholic steatohepatitis (NASH) patients: a connection between endogenous alcohol and NASH. *Hepatology* 2013;57:601–609.
[31] Shen B, Wang J, Guo Y, et al. Dextran sulfate sodium salt-induced colitis aggravates gut microbiota dysbiosis and liver injury in mice with non-alcoholic steatohepatitis. *Front Microbiol* 2021;12:756299.
[32] Boursier J, Mueller O, Barret M, et al. The severity of nonalcoholic fatty liver disease is associated with gut dysbiosis and shift in the metabolic function of the gut microbiota. *Hepatology* 2016;63:764–775.
[33] Panasevich MR, Meers GM, Linden MA, et al. High-fat, high-fructose, high-cholesterol feeding causes severe NASH and cecal microbiota dysbiosis in juvenile Ossabaw swine. *Am J Physiol Endocrinol Metab* 2018;314:E78–E92.
[34] Zhang X, Coker OO, Chu ES, et al. Dietary cholesterol drives fatty liver-associated liver cancer by modulating gut microbiota and metabolites. *Gut* 2021;70:761–774.
[35] Wang Q, Wang C, Abdullah, et al. Hydroxytyrosol alleviates dextran sulfate sodium-induced colitis by modulating inflammatory responses, intestinal barrier, and microbiome. *J Agric Food Chem* 2022;70:2241–2252.
[36] Lordan R, Tsoupras A, Zabetakis I, et al. Forty years since the structural elucidation of platelet-activating factor (PAF): historical, current, and future research perspectives. *Molecules* 2019;24:4414.
[37] Marrache AM, Gobeil F, Jr., Bernier SG, et al. Proinflammatory gene induction by platelet-activating factor mediated *via* its cognate nuclear receptor. *J Immunol* 2002;169:6474–6481.
[38] Yin H, Shi A, Wu J. Platelet-activating factor promotes the development of non-alcoholic fatty liver disease. *Diabetes Metab Syndr Obes* 2022;15:2003–2030.
[39] Pavlova T, Vidova V, Bienertova-Vasku J, et al. Urinary intermediates of tryptophan as indicators of the gut microbial metabolism. *Anal Chim Acta* 2017;987:72–80.
[40] Paulusma CC, Lamers WH, Broer S, et al. Amino acid metabolism, transport and signalling in the liver revisited. *Biochem Pharmacol* 2022;201:115074.

[41] Hu C, Li H, Wu L, et al. Metabolic profiling of 19 amino acids in triptolide-induced liver injured rats by gas chromatography-triple quadrupole mass spectrometry. *Hum Exp Toxicol* 2021;40:1685–1697.
[42] Men L, Wang Z, Gou M, et al. Metabolomics and targeted amino acid analysis reveal the liver protective effect of arginyl-fructosyl-glucose from red ginseng on acute liver injury in mice. *J Funct Foods* 2023;103:105473
[43] Marsh DC, Vreugdenhil PK, Mack VE, et al. Glycine protects hepatocytes from injury caused by anoxia, cold ischemia and mitochondrial inhibitors, but not injury caused by calcium ionophores or oxidative stress. *Hepatology* 1993;17: 91–98.
[44] Barakat HA, Hamza AH. Glycine alleviates liver injury induced by deficiency in methionine and or choline in rats. *Eur Rev Med Pharmacol Sci* 2012;16:728–736.
[45] Hua H, Xu X, Tian W, et al. Glycine alleviated diquat-induced hepatic injury *via* inhibiting ferroptosis in weaned piglets. *Anim Biosci* 2022;35:938–947.